International Journal of Modern Physics D

RADIATIVE PROCESSES IN JETS

Gabriela S. Vila

Instituto Argentino de Radioastronomía, CCT La Plata (CONICET)
Casilla de Correo 5 (1894), Villa Elisa, Buenos Aires, Argentina
gvila@iar-conicet.gov.ar

Received 10 December 2009
Revised 26 December 2009
Communicated by Managing Editor

Relativistic jets and collimated outflows are ubiquitous phenomena in astrophysical settings, from young stellar objects up to Active Galactic Nuclei. The observed emission from some of these jets can cover the whole electromagnetic spectrum, from radio to gamma rays. The relevant features of the spectral energy distributions depend on the nature of the source and on the characteristics of the surrounding environment. Here I review the main physical processes that command the interactions between populations of relativistic particles locally accelerated in the jets, with matter, radiation and magnetic fields. Special attention is given to the conditions that lead to the dominance of the different radiative mechanisms. Examples from various types of sources are used to illustrate these effects.

Keywords: Radiation mechanisms: non-thermal.

1. Introduction

Non-thermal radiation in jets is produced by interaction of relativistic particles with target fields of different nature. A number of processes can accelerate electrons and protons up to energies much larger than their rest mass energy. Relativistic particles can gain energy through diffusive shock acceleration[1], but other processes like the so-called converter mechanism[2] can be effective as well. These type of acceleration processes are interesting since they yield a power-law particle injection spectrum, $Q \propto E^{-\alpha}$. The presence of relativistic particles with a power-law energy distribution can be inferred in many cases from the observed emission of jets, typically from the synchrotron spectrum.

The target fields against which the relativistic particles interact depend on the nature of the source and its surroundings. They can be internal or external to the jet. Examples of external fields are stellar winds and radiation, photons from an accretion disc or corona and matter in the interstellar medium or nearby clouds. The jet radiation and co-moving matter field are possible internal targets, as well as the jet magnetic field.

2. Some basic concepts

Any process of interaction can be characterized by its cross section and inelasticity coefficient. The cross section σ is related to the probability of interaction; the inelasticity κ is defined as the fraction of the energy of the most energetic particle that is lost in the collision, $\kappa = \Delta E/E$. From these two quantities and the density n of the target field, it is possible to estimate the cooling rate of the process, $t^{-1} = -\dot{E}/E \approx c\,\kappa\,\sigma\,n$. This quantity is useful since it allows to asses which are the most relevant energy loss channels for the relativistic particles, among several competing processes. The maximum particle energy can also be estimated equating the cooling rate to the corresponding acceleration rate, as far as size constraints are satisfied.

To calculate the radiative output of any interaction mechanism it is necessary to know the energy distribution of the relativistic particles. The latter can be obtained solving the transport equation under the appropriate assumptions[3]. In the simplest case of an homogeneous region and neglecting particle escape[a], the steady-state particle distribution $N(E)$ [erg^{-1} cm^{-3}] is given by

$$N(E) = \left|\frac{dE}{dt}\right|^{-1} \int_E^{E_{\max}} Q(E')\,dE'. \tag{1}$$

From this expression it is readily seen that due to the effect of the energy losses, the functional form of $N(E)$ may not always reproduce that of the injection. Nevertheless, if $Q(E)$ is a power-law so is in general $N(E)$.

3. Non-thermal radiative processes in jets

3.1. *Interaction with magnetic fields*

3.1.1. *Synchrotron radiation*

Magnetic fields are a fundamental ingredient of jet formation and collimation, and particle acceleration. Synchrotron radiation is therefore almost an unavoidable cooling channel for energetic particles in jets. For a particle of mass m and energy E in a magnetic field B, the synchrotron energy loss rate is given by[4]

$$-\frac{dE}{dt} = \frac{4}{3}\frac{c\sigma_{\rm T}U_{\rm B}}{m_e^2c^4}\left(\frac{m_e}{m}\right)^4 E^2. \tag{2}$$

Here $U_{\rm B} = B^2/8\pi$ is the magnetic energy density, m_e is the electron mass and $\sigma_{\rm T}$ is the Thomson cross section. This expression is valid in the "classical" regime, $EB \ll m_e c^2 B_{\rm cr} \approx 10^7$ TeV G, where $B_{\rm cr} = m_e^2c^3/e\hbar \approx 4\times10^{13}$ G. When approaching this critical value quantum effects are not negligible. The energy of the emitted photons can be a large fraction of the particle energy, and other processes such as photon pair production ($\gamma + B \rightarrow e^+e^- + B$) become possible. These effects are

[a]Particles can be removed simply by escape from the source but also by decay.

not accounted for in the classical theory which, for instance, does not predict a cutoff in the synchrotron emission at the particle energy. Suitable expressions for the modified synchrotron radiation formulae are given, for example, by Refs. 5 and 6. In astrophysical environments such strong magnetic fields and high particle energies are not usually found, so the standard formalism can be safely applied in most cases. However, extreme physical conditions can occur in magnetars, highly magnetized accretion discs or the core of a collapsar. Thus, a quantum treatment is mandatory.

Synchrotron radiation is a very fast cooling channel for light particles like the electrons. The mass ratio in Eq. (2) strongly suppresses the efficiency of the process for more massive particles. For protons, for example, synchrotron losses are $(m_p/m_e)^4 \approx 10^{13}$ times slower than for electrons.

The spectral index of the particle distribution can be inferred from the observed synchrotron spectrum. If $N(E) \propto E^{-p}$, the synchrotron emissivity is $P_{\rm sy} \propto E_\gamma^{-(p-1)/2}$. Notice that p must not necessarily be equal to the injection spectral index. Using Eq. (2) and $Q \propto E^{-\alpha}$, Eq. (1) yields $p = \alpha + 1$. In those energy ranges where synchrotron losses dominate the cooling, the particle spectrum steepens.

Electron synchrotron radiation is detected from most sources with jets. As it is shown in Ref. 7, the approximately flat radio spectrum observed in AGN jets can be explained as the superposition of synchrotron components emitted in different regions of an expanding outflow. The presence of jets in microquasars (MQs) is also revealed by synchrotron radio emission from relativistic electrons[8]. Non-thermal radiation at radio frequencies has been detected as well from the radio lobes in Young Stellar Objects (YSOs)[9]. In these systems electrons are accelerated through shocks at the jet termination points, where the outflow is halted by the pressure of the molecular cloud in which the object is embedded. Figure 1 shows some examples of radio images of the jets in these three type of systems.

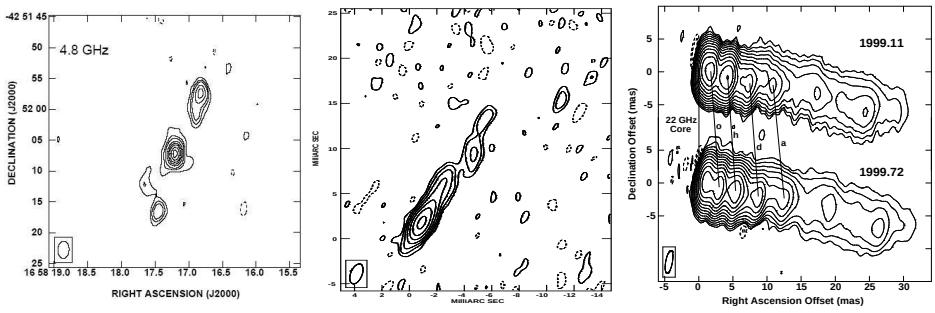

Fig. 1. Left: 4.8 GHz map of the triple radio source in the YSO IRAS 16547-4247. From Ref. 9. Center: radio image at 8.4 GHz of the jets in the MQ Cygnus X-1. From Ref. 11. Right: VLBI image at 43 GHz of the jet in the AGN 3C 120 in two different epochs. From Ref. 12.

Although in general synchrotron radiation is not an efficient colling process for

protons, it can become relevant in some sources if protons are very energetic. Ref. 13 presents a proton synchrotron model for the emission from knot A1 in the quasar 3C 273. For a magnetic field in the knot (size $\sim$ 1 kpc) of a few mG, protons are able to reach energies $E_p \approx 10^{18-20}$ eV. If the total power injected in relativistic protons is $L_p \approx 10^{45-47}$ erg s^{-1}, the observed spectrum from radio to X-rays is very well reproduced by the model. Synchrotron radiation of protons can also be relevant in proton-dominated jets in microquasars if the magnetic field is strong, see Ref. 22.

3.2. *Interaction with radiation fields*

3.2.1. *Inverse Compton scattering*

Inverse Compton scattering (IC) is an efficient radiation mechanism in many high-energy sources. The IC energy loss rate for an electron[b] of energy E in a photon field of energy density $U_{\rm ph}$ is[15]

$$-\frac{dE}{dt} = \frac{c\sigma_{\rm T}}{m_e^2 c^4} U_{\rm ph} E^2 F_{\rm KN}. \tag{3}$$

The expressions for the IC and synchrotron cooling rates are very similar; this can be understood if synchrotron emission is thought as scattering of virtual photons of the magnetic field. IC scattering also can proceed in the classical (Thomson) or in the quantum (Klein-Nishina, KN) regimes; the passage from one regime to another is accounted for by the function $F_{\rm KN}$ in Eq. 3. Unlike non-classical synchrotron radiation, however, the conditions for KN scattering are more frequently found in astrophysical environments.

In the Thomson regime ($\sigma_{\rm IC} \approx \sigma_{\rm T}$ and $F_{\rm KN} \approx 1$) the scattered photon carries away only a small fraction of the electron energy. In the KN regime energy losses are said to be "catastrophic": electrons can lose almost all their energy in a single collision. However, $\sigma_{\rm IC} \ll \sigma_{\rm T}$ and $F_{\rm KN} < 1$, so the energy loss rate decreases. As a result, electrons cool almost completely in a single interaction but at the same time collisions are less frequent. In this regime, the continuous approximation of Eq. 3 for the cooling rate is not strictly valid. Nevertheless, as shown in Ref. 14, it is in general accurate enough for most calculations.

When IC losses dominate, the steady-state electron energy distribution can display two breaks. At low energies, for those particles that cool in the Thomson regime, $N(E)$ is steeper than the injection, $N(E) \propto E^{-(\alpha+1)}$. On the other hand, the high-energy part of the distribution hardens again and mimics the injection $N(E) \propto E^{-\alpha}$. However, due to the combination of the two effects mentioned above, this break does not show in the photon spectrum that presents no noticeable break. These subtleties are extensively discussed in very interesting study of the consequences of IC cooling

[b]Proton IC scattering is also possible, but it is very inefficient compared to other cooling channels.

in the KN regime in radiation dominated environments[c] presented in Ref. 15.

IC scattering can contribute significantly to the high-energy emission spectrum in high-mass microquasars (HMMQs). In these systems there are a number of components that can provide target photons. Several IC emission models are presented in Ref. 16 for different dominant internal or external target fields: accretion disc, corona or stellar photons[d], and the jet internal synchrotron field[e]. Depending on the model the IC luminosity at ~ 1 GeV can reach $\sim 10^{35}$ erg s^{-1}, see Fig. 2.

In HMMQs with very luminous companions part of the high-energy emission can be absorbed in the stellar radiation field. If the magnetic field is low enough[f] an electromagnetic cascade may develop: high-energy photons from the jet annihilate with stellar photons to produce electron-positron pairs, that in turn up-scatter stellar photons that annihilate again, etc. IC cascades in HMMQs are studied, for example, in Ref. 18. The net result of the cascade is to distort the shape of the primary spectrum, suppressing part of the jet high-energy emission and channeling the energy to lower frequencies.

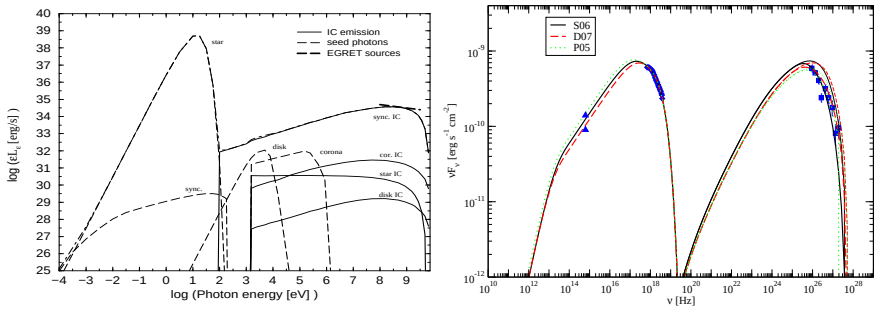

Fig. 2. Left: emission from a HMMQ predicted by the model of Ref. 16. In this scenario the high-energy emission is due to SSC. The model reproduces the observed spectrum of some EGRET sources. Right: models for the synchrotron and SSC emission from the 2001 flare of the BL Lac Object Mkn 421. Thin curves are unabsorbed spectra, whereas thick curves were calculated including $\gamma\gamma$ absorption in the jet internal radiation field and in the background intergalactic light. From Ref. 19.

IC emission also contributes to the continuum emission of blazars. The spectrum shows a double-peaked structure: the low-energy peak is due to synchrotron radiation and the high-energy peak due to IC scattering. External target photon fields can be supplied, for example, by accretion disc emission, radiation reprocessed

[c]Since $F_{\rm KN} \leq 1$, synchrotron losses always dominate over IC losses in magnetically dominated regions ($U_{\rm B} > U_{\rm ph}$).

[d]External IC is not an efficient radiation process in low-mass microquasars since external fields are in general very faint.

[e]In this particular case IC scattering is called *Synchrotron Self Compton* (SSC).

[f]As shown in Ref. 17 a high value of the magnetic field can suppress the cascade. Electrons cool rapidly through synchrotron radiation without emitting photons energetic enough to create another generation of pairs.

in clouds, and even by the cosmic background photons. Nevertheless, the internal low-energy synchrotron photon field is in general the most relevant target and the SSC contribution is the most important one. Figure 2 shows some SSC model fits to the spectrum of Mkn 421 obtained with the model of Ref. 19.

3.2.2. *Photohadronic interactions ($p\gamma$)*

Relativistic protons interact with radiation mainly through direct pair creation

$$p + \gamma \rightarrow p + e^+ + e^-, \tag{4}$$

and pion production[g]

$$p + \gamma \rightarrow p + \pi^0 + a(\pi^+ + \pi^-) \qquad p + \gamma \rightarrow n + \pi^+ a\pi^0 + b(\pi^+ + \pi^-). \tag{5}$$

The integers a and b are the pion multiplicities. Neutral pions then decay to two gamma rays and charged pions in muons (which yield electron-positron pairs and neutrinos) and muon neutrinos.

Direct pair creation is possible for photon energies $E_{\rm ph} \gtrsim 1$ MeV measured in the proton rest frame. The cross section of this process is relatively large, $\sigma_{p\gamma}^{e^\pm} \approx 1$ mb at the threshold, but the inelasticity is small $\kappa_{p\gamma}^{e^\pm} \approx 10^{-3}$. The photon energy threshold for pion production is $E_{\rm ph} \approx 140$ MeV. The cross section is smaller than for photopair production, $\sigma_{p\gamma}^{\pi} \approx 0.1 - 0.5$ mb, but the inelasticity is significantly larger, $\kappa_{p\gamma}^{\pi} \approx 0.2 - 0.6$. Low energy protons then cool mainly by pair production, but as soon as the energy threshold for pion creation is reached, the latter process completely dominates the cooling.

Photohadronic interactions can be an important radiative mechanism in sources with a high photon density. Ref. 22 presents a model for low-mass microquasar (LMMQ) jets that predicts very high-energy electromagnetic emission due to $p\gamma$ collisions. In this model the magnetic field near the base of the jet is intense, and relativistic electrons cool completely by synchrotron radiation providing a dense target photon field. Electromagnetic emission is produced through π^0 decay and also by synchrotron radiation of pairs injected via $\pi^\pm$ decay or direct pair production. Depending on the model parameters, luminosities of $\sim 10^{35-36}$ erg s^{-1} above ~ 1 TeV are predicted. In some cases, however, most of the radiation above ~ 1 GeV is absorbed due to $\gamma\gamma$ annihilation in the electron synchrotron field.

A signature of high-energy proton interactions is the production of neutrinos; these are injected by the decay of charged mesons and muons. Magnetic field effects on neutrino production in MQs have been extensively studied in Ref. 23. These authors show that when energy losses (mainly synchrotron) of pions and muons are taken into account, the high-energy neutrino emission is significantly reduced

[g]A proton is converted into a neutron in about a half of the collisions.

compared to the case without cooling. In some models the predicted fluence above $E_\nu \sim 1$ TeV can fall well below the sensitivity limits of km^3 detectors.

Neutrino emission in AGNs due to $p\gamma$ interactions has been considered in several works. In the frame of the Proton Synchrotron Blazar model, Ref. 24 presented a study of the neutrino production in blazars caused by collisions of relativistic protons with the low-energy electron synchrotron field. A significant neutrino emission, of the same order of the gamma-ray emission, is predicted for Low-energy cutoff BL Lac objects (LBLs). A different proton blazar model is presented in Ref. 25, where the accretion disc photon field is also included as target. An interesting aspect of this model is that it takes into account the production of neutrons in photomeson interactions. Some neutrons can escape from the source and interact with photons far from the jet, yielding neutrinos but also gamma rays. These gamma-rays have a higher chance to escape without being absorbed than the ones produced in the inner jet, since they are created in a region of lower radiation density. These models, however, do not consider the effects of the magnetic field, which might be very significant.

Neutrino emission is also expected from Gamma Ray Bursts (GRBs). Refs. 26 and 27 present a model for neutrino production due to $p\gamma$ interactions in a collapsar jet. Target photons are supplied by the thermal radiation field of electrons, heated to very high energies by a reverse shock that propagates through the jet. The model yields a detectable flat neutrino flux above ~ 2 TeV. An interesting prediction is that the same neutrino flux would be expected from choked GRBs.

3.3. *Interaction with matter fields*

3.3.1. *Proton-proton interactions (pp)*

The collision of relativistic protons with low-energy protons creates neutral and charged pions,

$$p + p \rightarrow p + p + \pi^0 + a(\pi^+ + \pi^-) \qquad p + p \rightarrow p + n + \pi^+ + a\pi^0 + b(\pi^+ + \pi^-). \quad (6)$$

The cross section for this process is large, $\sigma_{pp} \approx 30$ mb at the threshold energy $E_p \approx 1.2$ GeV (an useful parametrization of the cross section can be found in Ref. 28). The total inelasticity of the process has also a high value, $\kappa_{pp} \approx 0.5$; approximately $\kappa_{pp}^{\pi} \approx 0.17$ of the relativistic proton energy is carried away by a single leading pion. The *pp* energy loss rate depends linearly on the proton energy,

$$-\frac{dE}{dt} = c n_{\rm H} \kappa_{pp} \sigma_{pp}(E_p) \propto E_p \ln(E_p). \quad (7)$$

Here $n_{\rm H}$ is the density of target protons. If *pp* collisions are the main cooling channel, it can be readily seen from Eq. 1 that for a power-law injection $Q(E_p) \propto E_p^{-\alpha}$ the proton distribution shares the same spectral shape, $N(E_p) \propto E_p^{-\alpha}$.

Proton-proton interactions can be a relevant mechanism of high-energy emission in "windy" HMMQs. The matter in the wind of the companion star provides a suitable target for the relativistic protons in the jets. A simple model for *pp* emission in HMMQs is presented in Ref. 29. Detectable gamma-ray luminosities of up to $\sim 10^{35-36}$ erg s^{-1} at $E_\gamma \sim 10$ GeV are obtained due to π^0 decay. In this model the wind is homogeneous. There is firm evidence, however, that stellar winds have a clumpy structure with condensations of high density. If a clump penetrates the jet, this may produce a high-energy flare via *pp* interactions between the high density matter in the clump and the relativistic protons in the outflow This has been recently studied in Ref. 32. These authors obtained *pp* luminosities of $\sim 10^{33}$ erg s^{-1} at $E_\gamma \gtrsim 1$ TeV for some models. The situation is far from simple, since shocks form around and inside the clump, which can even be destroyed during its passage through the jet.

Electromagnetic emission due to *pp* collisions can also be relevant in AGNs. Models for gamma-ray emission in *pp* interactions between relativistic protons in the jet and matter in clouds of the Broad Line Region are presented, for example, in Ref. 33 and, more recently in Ref. 34 .

3.3.2. *Relativistic Bremsstrahlung*

The Bremsstrahlung energy loss rate for an electron of Lorentz factor $\gamma_e = E_e/m_e c^2$ in a completely ionized plasma of charge Z and density n_0 is

$$-\frac{dE}{dt} = 4\alpha\, c\, n_0 Z^2 \left[\ln(\gamma_e + 0.36)\right] E_e. \tag{8}$$

In general, Bremsstrahlung losses dominate for electron energies $E_e \gtrsim 700 m_e c^2$; at lower energies electrons cool mainly by ionization. Bremsstrahlung losses are catastrophic, the electron losses most of its energy in each interaction. Due to the linear dependence on the energy of the loss rate the steady-state particle distribution has the same spectral index than the injection.

Bremsstrahlung emission can contribute significantly to the spectrum of sources embedded in high-density environments. The non-thermal emission from some supernova remnants is thought to be produced through relativistic Bremsstrahlung; see, for example, Ref. 30 for the case of SNR IC 443[h]. In systems with jets, high matter densities are found in the molecular clouds that surround YSOs. In the particular case of the source IRAS 16547-4227, it was shown in Ref. 32 that the Hydrogen density in the shocked radio lobes may be as high as $n_0 \approx 2 \times 10^4$ cm^{-3}. In this model, Bremsstrahlung emission from non-thermal electrons with maximum energies $E_e \approx 1$ TeV is the main contribution to the gamma-ray spectrum between $\sim$1 MeV and $\sim$10 GeV.

[h]The Bremsstrahlung origin of non-thermal radiation in this system has been recently questioned in the light of its detection with the MAGIC telescope at gamma-rays[31]. High-energy radiation may be produced via *pp* interactions between protons accelerated in the SNR and the material in the surrounding molecular cloud.

4. Concluding remarks

The broadband non-thermal spectrum from jets can be complex since several radiative processes can contribute to the spectral energy distribution in different energy ranges. The relative importance of each contribution depends on the outflow environment and on some not well-known parameters such as the value of the magnetic field, the distribution of the relativistic particles or the hadronic content of the jets. In the near future, detailed multiwavelength observations together with more refined theoretical models will contribute to a better understanding of the physical conditions in astrophysical outflows.

Acknowledgments

I thank the organizers of the HEPRO II meeting for the opportunity to present this review. This work was supported by ANPCyT through grant PICT-2007-00848 BID 1728/OC-AR.

References

1. L O'C Drury *Rep. Prog. Phys.* **46** (1983) 973.
2. E.V. Derishev, F.A. Aharonian, V.V. Kocharovsky and Vl.V. Kocharovsky *Phys. Rev. D* **68** (2003) 043003.
3. V.L. Ginzburg and S.I. Syrovatskii *Origin of Cosmic Rays* (Macmillan, New York, 1964).
4. G.R. Blumenthal and R.J. Gould *Rev. Mod. Phys.* **42** (1970) 237.
5. J.J. Brainerd and Q.D. Lamb *ApJ* **313** (1987) 231.
6. M.G. Baring *MNRAS* **235** (1988) 51.
7. R.D. Blandford and A. Königl *ApJ* **232** (1979) 34.
8. I.F. Mirabel, L.F. Rodriguez, B. Cordier and F. Lebrun *Nature* **358** (1992) 215.
9. G. Garay, K.J. Brooks, D. Mardones and R.P. Norris *ApJ* **587** (2003) 739.
10. K.J. Brooks, G. Garay, D. Mardones and L. Bronfman *ApJ* **594** (2003) L131.
11. A. M. Stirling, R. E. Spencer, C. J. de la Force, M. A. Garrett, R. P. Fender and R. N. Ogley *MNRAS* **327** (2001) 1273.
12. P.E. Hardee, R.C. Walker and J.L. Gómez *ApJ* **620** (2005) 646.
13. F.A. Aharonian *MNRAS* **332** (2002) 215.
14. D. Khangulyan and F.A. Aharonian, *AIP Conference Proceedings* **745** (2005) 359.
15. R. Moderski, M. Sikora, P. Coppi and F. Aharonian *MNRAS* **363** (2005) 954.
16. V. Bosch-Ramon, G.E. Romero and J.M. Paredes *A&A* **429** (2005) 267.
17. D. Khangulyan, F.A. Aharonian and V. Bosch-Ramon *MNRAS* **383** (2009) 467.
18. M. Orellana, P. Bordas, V. Bosch-Ramon, G.E. Romero and J.M. Paredes *A&A* **476** (2007) 9.
19. F.D. Justin, C.D. Dermer and M. Böttcher *ApJ* **686** (2008) 181.
20. M. Begelman, B. Rudak and M. Sikora *ApJ* **362** (1990) 38.
21. S.R. Kelner and F.A. Aharonian *Phis. Rev. D* **78** (2008) 034013.
22. G.E. Romero and G.S. Vila *A&A* **485** (2008) 623.
23. M.M. Reynoso and G.E. Romero *A&A* **493** (2008) 1.
24. A. Mücke and R.J. Protheroe, Neutrino emission from HBLs and LBLs in *Proc. ICRC 2001*, p. 1.
25. A.M. Atoyan and C.D. Dermer *ApJ* **586** (2003) 79.
26. P. Mészáros and E. Waxman *Phys. Rev. Lett.* **87** (2001) 171102.

27. E. Waxman and P. Mészáros *ApJ* **584** (2003) 390.
28. S.R. Kelner, F.A. Aharonian and V.V. Bugayov *Phis. Rev. D* **74** (2006) 034018.
29. G.E. Romero, D.F. Torres, M.M. Kaufman Bernadó and I.F. Mirabel *A&A Letters* **410** (2003) L1.
30. A.M. Bykov, R.A. Chevalier, D.C. Ellison and Y.A. Uvarov *ApJ* **538** (2000) 203.
31. J. Albert et al. *ApJ* **664** (2007) L87.
32. A.T. Araudo, V. Bosch-Ramon and G.E. Romero *A&A* **503** (2009) 673.
33. A. Dar and A. Laor *ApJ* **478** (1997) L5.
34. A.T. Araudo, V. Bosch-Ramon and G.E. Romero, *IJMP D*, this issue.